Journal of the Korean Nuclear Society
Volume 12, *Number* 4, *December*, 1980

《**Original**》

An In-Core Fuel Management Analysis for a PWR Power Plant*

Chang Hyo Kim, Chang Hyun Chung and Jin Soo Kim

Seoul National University

(Received November 23, 1980)

ABSTRACT

The TDCORE and the RELOAD-Ⅱ codes are adopted in an attempt to establish a simplified computational system for the in-core fuel management decisions of a PWR. The TDCORE is being used to simulate the power and burnup behavior of the Gori unit 1 PWR during the fuel cycle 1 through the cycle 5. The validity of the TDCORE code is also presented by comparing the TDCORE prediction with the in-core measurements. The RELOAD-Ⅱ code is used to determine the optimum fuel loading pattern which is one of the most important decisions of the Gori unit 1 reactor. The utility and applicability of two codes for the fuel management analyses are described.

요 약

가압경수로의 핵연료관리 정책 결정에 사용될 간편한 해석체재를 수립하기 위한 시도로서 TDCORE 및 RELOAD-Ⅱ 전산코드를 채택했다. TDCORE 전산코드는 고리 1호기에서 제 5주기까지의 노심내 출력 및 연소도이력과정을 묘사하는데 사용했으며, 이 코드의 타당성은 노심내 측정치와의 비교를 통해 입증했다. RELOAD-Ⅱ 전산코드는 고리 1호기의 중요한 핵연료관리 정책사항중의 하나인 연료집합체의 최적 재장전모형을 선정하는데 이용했다. 핵연료관리 해석에 대한 두 전산코드의 용도 및 응용에 관해 기술했다.

1. Introduction

In-core fuel management for the multi-cycle fueling PWR concerns with the optimum decisions upon the number and enrichment of fresh fuel assemblies to be charged, selection of assemblies for discharge, and the allocation of the individual fuel assemblies into the core[1~3]. The optimum decisions upon these parameters can be marketed from the reactor vendor or the fuel supplier, yet it is desirable for the instituter responsible for the plant operation to establish a comprehensive fuel management computational system either to make its own fuel management decisions or to evaluate and select the optimum alternatives.

As an initial attempt toward this objective

* This work was supported by the Ministry of Education, Republic of Korea.

we have developed a simplified fuel management computational system[4]; the TDCORE and the RELOAD-Ⅱ codes. TDCORE is a two-dimensional, two-group diffusion theory code programmed in the spirit of Bφrrensen reactor model[5]. RELOAD-Ⅱ is the fuel assembly loading pattern search code based on the assembly shuffling logic of Stout and Rovinson for the minimization of the radial power peaking factor[6].

This paper is intended to demonstrate the applicability and the utility of two codes for the fuel management computations of the 595 Mw(e) Gori unit 1 PWR. The specific numerical results are the power and burnup performance for each fuel cycle from 1 to 5 and the optimum fuel loading pattern of the individual cycle when the batch-by-batch refueling scheme is assumed. In the following we describe briefly the TDCORE and the RELOAD-Ⅱ code and present results of fuel management computations for the Gori core.

2. Description of Computational System

Two types of computations are attempted in this study; simulation of the core power and burnup behavior and determination of the optimum fuel loading pattern. Computations are carried out on the basis of two principal computer codes; TDCORE and RELOAD-Ⅱ. A brief description is given below.

The TDCORE code is a two-dimensional, two-group diffusion theory code designed to simulate the neutronic parameters of a large PWR core such as the XY power distribution, burnup history of the individual fuel assembly, and the critical boron concentration with a reasonable computing time and accuracy. The code incorporates two basic approximations suggested by Bφrrensen[5] for a simplified coarse-mesh finite difference relation of the group diffusion equations. One is to approximate the coupling coefficients between the group fluxes at the centers of two adjacent i and j nodes, a_g^{ij}, by

$$a_g^{ij}=\frac{D_{gi}\cdot D_{gj}}{D_{gi}+D_{gj}}\simeq\frac{1}{2}\sqrt{D_{gi}\cdot D_{gj}} \tag{1}$$

The other is to approximate the volume-averaged group flux, ϕ_{gi}, by

$$\phi_{gi}=a_g\phi_{gi}+\frac{1-a_g}{4}\sum_i\phi_j^{gi}, \tag{2}$$

where ϕ_{gi} and ϕ_j^{gi} are the group flux at the center of node i and the group flux at the interface between nodes i and j, respectively and a_g is the appropriate weighting constant for the flux of group g. One specific feature of the TDCORE is that it uses the albedo-type boundary condition,

$$\phi_g(r_s)=\alpha_g J_g(r_s), \tag{3}$$

at the core-reflector interface with α_g being the albedo constant of group g flux at the core-reflector interface denoted by r_s. This boundary condition makes it possible to avoid explicit computations of group fluxes in the reflector region, and thereby saves a lot of computer memory and computing time as well.

The RELOAD-Ⅱ code is the assembly-by-assembly reload pattern search code for the minimization of the radial power peaking factor. The RELOAD-Ⅱ code starts with an arbitrary trial fuel loading pattern and performs shuffling of fuel assemblies in three steps according to the position interchange rules of two fuel assemblies developed by Stout and Robinson[6], The first step is to exchange the peak assembly with the largest radial peaking factor in the entire core with an assembly which obeys the shuffling logic and is closer to the one with

minimum peaking factor among eight fuel assemblies in the close contact with the peak assembly. This step is intended to keep the highly reactive fuel assemblies as far apart as possible, and terminates when interchange of two fuel assemblies results in no further reduction in the power peaking factor for the core. The second step is to exchange the highest power assembly among 8 fuel assemblies surrounding the peak assembly which has been moved by the first step with the lowest power assembly in the rest of the core. The third step is similar to the second step, but the highest power assembly is chosen among 16 fuel assemblies in the outermost shell of the 5x5 array around the peak assembly. The last two steps are designed to allocate the least reactive fuel assemblies around the most reactive fuel assemblies. Implementation of these steps in the RELOAD-Ⅱ code is described in detail in ref. 4.

3. Numerical Results and Discussion

3.1. Validity of the TDCORE code

The TDCORE code is instrumental in performing the neutronic computations required to simulate the power and the burnup performance in a PWR core and determine the optimum loading pattern as well. Therefore, it is the important first step to establish the validity of the TDCORE code before using it for various computations. This can be done by comparison of the TDCORE predictions with the in-core measurements.

In Fig. 1 is shown an octant of the first core for the 595 Mw(e) Gori unit 1 PWR[7] which is chosen as a reference system in this study. Each square represents one fuel assembly. The top line in the square stands

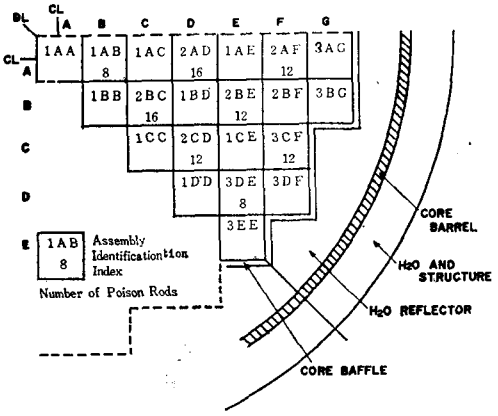

Fig. 1. Octant-Core of Gori Unit No. 1 PWR

for the assembly identification index in which the numerical character designates the batch number and two alphabets the XY coordinates. The figures under the assembly identification index denote the number of burnable poison rods contained in the corresponding assembly.

The TDCORE code requires a set of input data which include the model constants and the assembly-homogenized two-group cross sections. In Table 1 the model constants of the code are listed. The numerical values for a_1 and a_2 are those recommended by Bφrrensen. The albedo constant for fast flux, α_1 is obtained from Henry's method[8] The albedo constant for thermal flux, α_2 is obtained by matching the CITATION-computed thermal flux distribution[9] with the TDCORE-computation. As for the assembly-homogenized two-group cross sections, we take the group constants[10] which are obtained from a combination of LEOPARD super cell and CITATION computations for various fuel burnup steps, and fitted them to the

Table 1. Model Constants of the TDCORE Code

Model Constants	a_1	a_2	α_1(a)	α_2
Numerical Value	0.3	0.7	6.5	0.6

(a) α_1=7.5 for cycles 2 to 5

Table 2. Two-Group Constants for Batch 1 Fuel Assembly without Burnable Poison Rods[a]

Two-Group Constants / Expansion Coefficients	Σ_{tr}		Σ_a		$\nu\Sigma_f$		σ_B[b]		κ[c]		Σr
	$g=2$	$g=1$	$g=2$	$g=1$	$g=2$	$g=1$	$g=2$	$g=1$	$g=2$	$g=1$	
C_1	5.4756 ($\times10^{-1}$)	1.4340	1.3912 ($\times10^{-1}$)	2.6195 ($\times10^{-2}$)	1.8120 ($\times10^{-1}$)	5.4371 ($\times10^{-3}$)	3.9721 ($\times10^{3}$)	4.5937 ($\times10^{1}$)	2.3703 ($\times10^{-12}$)	6.6686 ($\times10^{-14}$)	1.7060 ($\times10^{-2}$)
C_2	−2.8427 ($\times10^{-6}$)	7.5860 ($\times10^{-7}$)	6.6123 ($\times10^{-6}$)	1.7913 ($\times10^{-8}$)	8.6235 ($\times10^{-6}$)	−2.0572 ($\times10^{-8}$)	6.6988 ($\times10^{-3}$)	−5.7928 ($\times10^{-5}$)	8.5613 ($\times10^{-17}$)	−4.4815 ($\times10^{-19}$)	−3.0887 ($\times10^{-8}$)
C_3	5.5429 ($\times10^{-10}$)	8.5229 ($\times10^{-11}$)	−1.2074 ($\times10^{-9}$)	4.8050 ($\times10^{-12}$)	−1.3313 ($\times10^{-9}$)	−6.1993 ($\times10^{-12}$)	−1.2085 ($\times10^{-6}$)	−2.7000 ($\times10^{-8}$)	−1.4755 ($\times10^{-20}$)	−6.9359 ($\times10^{-23}$)	−2.0240 ($\times10^{-11}$)
C_4	−6.2319 ($\times10^{-14}$)	−2.0582 ($\times10^{-15}$)	1.2582 ($\times10^{-13}$)	−5.7594 ($\times10^{-16}$)	1.1802 ($\times10^{-13}$)	8.1293 ($\times10^{-16}$)	1.3876 ($\times10^{-10}$)	4.5150 ($\times10^{-12}$)	1.3208 (10^{-24})	1.0580 ($\times10^{-26}$)	3.1932 ($\times10^{-16}$)
C_5	3.7116 ($\times10^{-18}$)	−7.0076 ($\times10^{-19}$)	−7.6439 ($\times10^{-18}$)	2.3767 ($\times10^{-20}$)	−5.8527 ($\times10^{-18}$)	−4.8423 ($\times10^{-20}$)	−8.3005 ($\times10^{-15}$)	−3.0390 ($\times10^{-16}$)	−6.5574 ($\times10^{-29}$)	−7.0157 ($\times10^{-31}$)	−2.0176 ($\times10^{-19}$)
C_6	−8.5486 ($\times10^{-23}$)	3.6951 ($\times10^{-23}$)	1.8946 ($\times10^{-22}$)	−3.6851 ($\times10^{-25}$)	1.1604 ($\times10^{-22}$)	1.0858 ($\times10^{-24}$)	1.8863 ($\times10^{-19}$)	7.3731 ($\times10^{-21}$)	1.3039 ($\times10^{-33}$)	1.7281 ($\times10^{-35}$)	4.6094 ($\times10^{-24}$)
δ	1.1742 ($\times10^{-3}$)	−9.0830 ($\times10^{-4}$)	7.8633 ($\times10^{-4}$)	−5.6959 ($\times10^{-6}$)	6.9884 ($\times10^{-4}$)	−5.5318 ($\times10^{-6}$)	−6.7051 ($\times10^{1}$)	1.2590	5.2192 ($\times10^{-15}$)	−1.7889 ($\times10^{-16}$)	−6.0348 ($\times10^{-5}$)

(a) $\Sigma=C_1+C_2B+C_3B^2+C_4B^3+C_5B^4+C_6B^5+\delta$; δ is added only at BOC.
(b) σ_B=effective microscopic two-group cross section of boron-10
(c) κ=energy generated per fission.

Table 3. Comparison of the TDCORE and the CITATION Computations

Items	CITATION	TDCORE
Number of Nodes per Fuel Assembly (unknowns)	6x6 nodes (36)	1 node (6)
Effective Multiplication Factor (keff)	1.00078	0.99886
Fast Neutron Flux/Thermal Neutron Flux (at 1AA)	8.3037	8.4182
Fast Neutron Flux/Thermal Neutron Flux (at 3AG)	1.1405	1.1488
Fast Neutron Flux/Fast Neutron Flux (at 1AA) (at 3AG)	1.4093	1.3696
Thermal Neutron Flux/Thermal Neutron Flux (at 1AA) (at 3AG)	1.9359	1.8691
Computer Running Time (Seconds)	200	5

sixth order polynomial of the core burnup. In Table 2 are listed the expansion coefficients of the polynomial with regard to the two-group constants of batch 1 fuel assemblies without burnable poison rods. Similar tables for other types of fuel assemblies are obtained and given in ref. 4.

In Fig. 2 the assemblywise TDCORE power distribution is compared with the CITATION-predicted one at the biginning of cycle (BOC) of the Gori first core. In Table 3 the comparision of two calculations is summarized with regard to the computational accuracy and computer running time. The TDCORE code takes a relatively short computer time. It requires about 5 seconds for predicting the assemblywise power distribution on the CDC CYBER-73 computer, whereas the CITATION code requires about 200 seconds. The maximum discrepancy in the assemblywise power distribution is shown to be about 5.5%, which is acceptable for this kind of calculations. As for the effective multiplication factor, two compu-

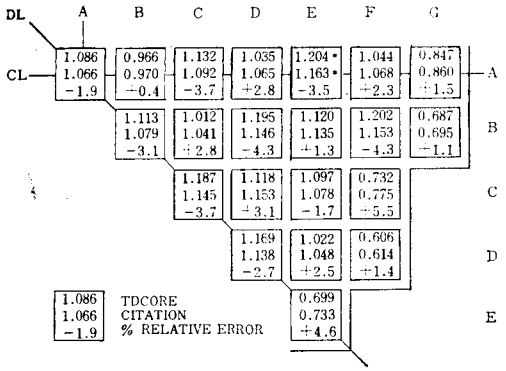

Fig. 2. Assemblywise Power Distribution at the BOC of the Gori Core

tations are shown to be in agreement with each other within 0.3%.

The validity of the TDCORE code can also be checked with the in-core measurents conducted by the Korea Electric Company (KECO) for the Gori unit 1 core[11]. In Fig. 3 the TDCORE computation is compared with the measurements for the assemblywise power distribution at the burnup step of

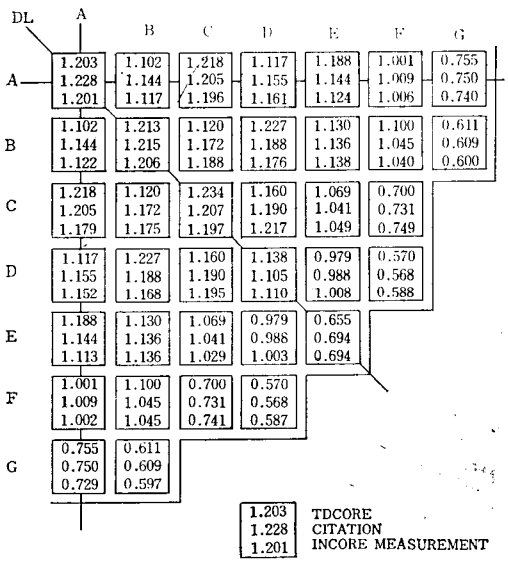

Fig. 3. Comparison of the TDCORE-predicted Assemblywise Power Distribution with the In-core Measurements at Burnup Step of 2629 MWD/MTU (Critical Boron Concentration: 900.2 ppm)

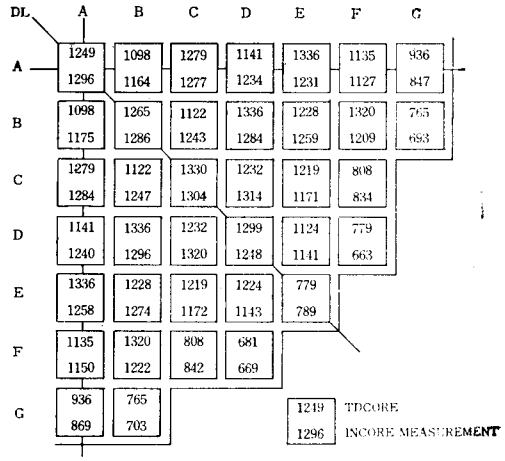

Batch	TDCORE	MEASUREMENTS
1	1271	1248
2	1208	1247
3	847	853

Fig. 4. Comparison of TDCORE-predicted Assemblywise Burnup Distribution with Measurements at the Burnup Step of 1110 MWD/MTU

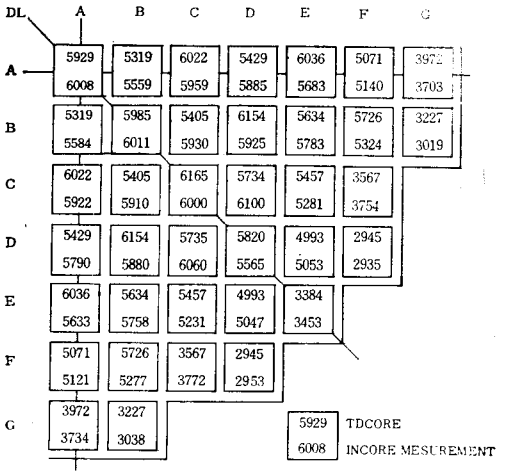

Batch	TDCORE	MEASUREMENT
1	5859	5714
2	5550	5711
3	3682	3674

Fig. 5. Comparison of TDCORE-predicted Assemblywise Burnup Distribution with Measurements at the Burnup Step of 5037 MWD/MTU

2926 MWD/MTU. Similar comparisions for the assemblywise burnup distribution at the burnup steps of 1110 and 5037 MWD/MTU are made in Figs. 4 and 5. In Fig. 6 the variation of the critical boron concentration with the core burnup is compared with the Westinghouse design data. It is observed that the overall agreeements of two predictions are fairly good.

3.2. First Cycle Depletion Analysis

The depletion characteristics of principal interest are the assemblywise core power and burnup distributions and the critical boron concentrations with the core burnup. Computations of these characteristics are carried out at the hot full power condition of the Gori unit 1 core with all the control rods out, using the TDCORE code.

The critical boron concertration is already shown in Fig. 6 as a function of the core burnup. Shown in Figs. 7 and 8 are the assemblywise core power and burnup distributions at the burnup step of 6000 MWD/MTU and at the end of cycle (EOC). The EOC corresponds to the core state in which the critical boron concentration reaches about 50 ppm.

It is indicated in Fig. 8 that the TDCORE-predicted discharge burnup of the Gori first cycle is 14160 MWD/MTU. This value is somewhat lower than the Westinghouse-predicted discharge burnup of 14650 MWD/

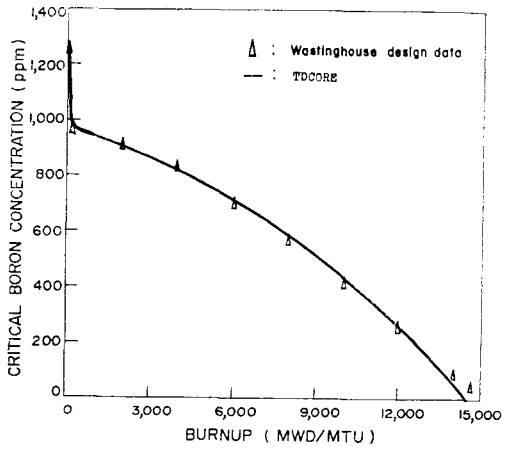

Fig. 6. Variation of Critical Born Concentration with Burnup by the First Cycle of the Gori Reactor

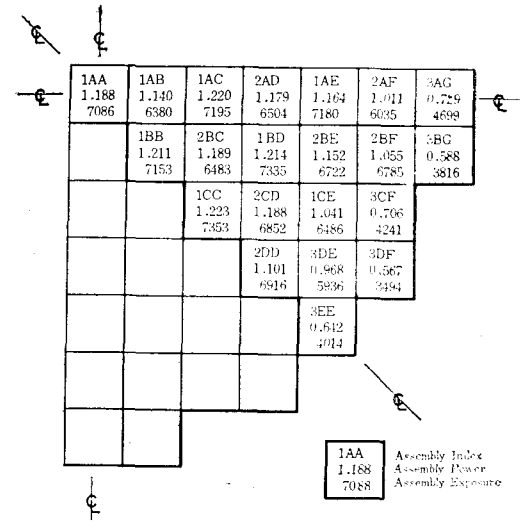

Fig. 7. The Assemblywise Core Power and Burnup Distribution at the Burnup Step of 6000 MWD/MTU, First Cycle

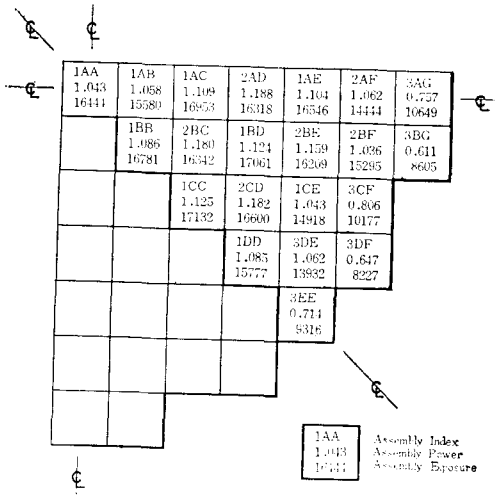

Fig. 8. The Assemblywise Core Power and Burnup Distribution at the Burnup Step of 14160 MWD/MTU, First Cycle

MTU[11]. But it is noted that the discrepancy by about 500 MWD/MTU is tolarable in view of our simple and fast two dimensional calculations in contrast to the detailed design analyses.

3.3. Optimum Fuel Loading Pattern of the 2nd Cycle

The planned refueling scheme of the Gori reactor was the scheme marketed by the Westinghouse in which the 40 batch 1 fuel assemblies are discharged and the 40 batch 4 fuel assemblies of 3.2w/o U-235 are newly charged. If this refueling scheme is assumed for the second cycle of the Gori reactor, the fuel assemblies subject to the loadinng pattern search via the RELOAD-Ⅱ code include one fuel assembly of the batch 1 and the batches 2, 3, and 4 fuel assemblies with 40 each.

Shown in Fig. 9 is a trial assembly loading pattern in which 121 fuel assemblies are arranged to maintain the octant-core symmetry. The radial power peak occurs at the fresh fuel assembly designated by 4DE with the peaking factor of 1.2556. The second highest peak occurs at the 3BG assembly with the peaking factor of 1.1910. In Fig. 10 the shuffling of fuel assemblies is depicted, as dictated by the RELOAD-Ⅱ code, toward the desired optimum power density distribution. The arrows in Fig. 10 indicate only the initial and the final positions of the fuel assembly movements. The number of trials that the positions of two fuel assemblies are interchanged in bringing the trial loading pattern to the optimum one via RELOAD-Ⅱ is a total of 29.

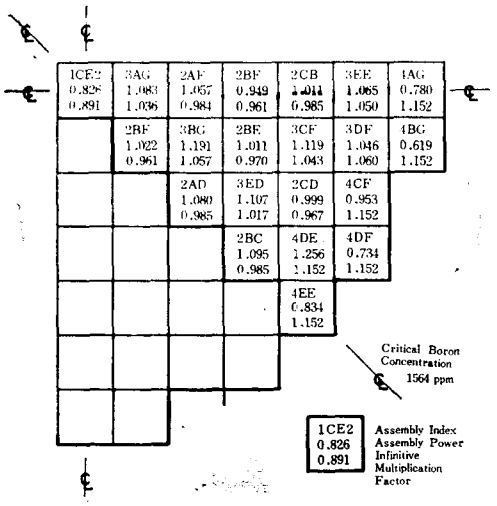

Fig. 9. Trial Fuel Assembly Loading Pattern of the Second-cycle Gori Core

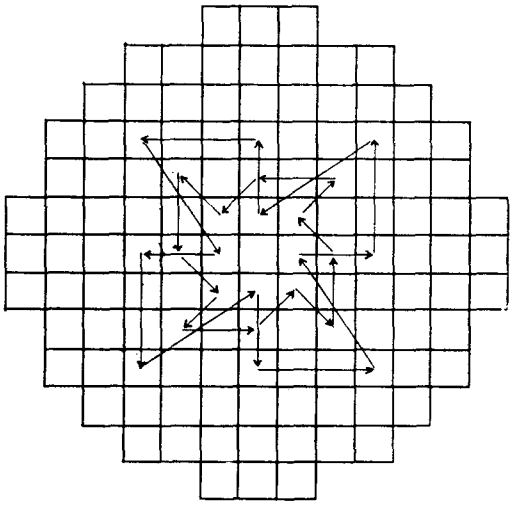

Fig. 10. Shuffling of Fuel Assemblies toward the Minimum Power Peak

The power distribution is presented in Fig. 11 for the optimum fuel loading pattern determined by the RELOAD-Ⅱ code. The power peak in this pattern occurs at the same fuel assembly in the trial pattern but the peaking factor reduced from 1.2556 to 1.2154. The second highest power peak in the optimum loading pattern also occurs at the same assembly in the trial pattern but its peaking factor decreased from 1.1910 to 1.7775. It is noted that these reductions in

peaking factors are due to the allocation of the least reactive fuel assembly around the most reactive fuel assembly and of the less reactive fuel assemblies around the more reactive fuel assemblies.

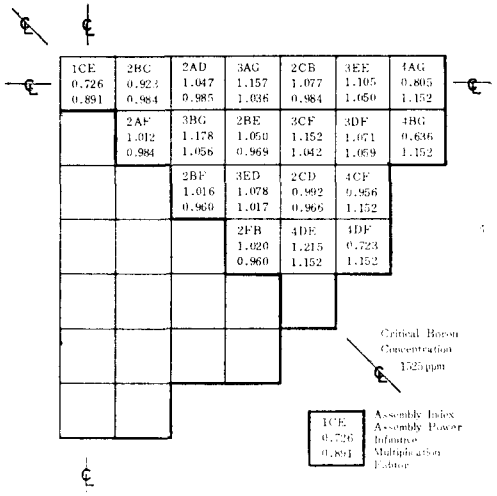

Fig. 11. Optimum Fuel Loading Pattern Determined by RELOAD-II

The final placement of each fuel assembly in the RELOAD-Ⅱ-predicted optimum pattern is dependent upon its initial location in the trial pattern. In other words, RELOAD-Ⅱ does not predict one unique pattern for many different trial loading patterns. Neverthless, it predicts the loading patterns whose radial power peaking factor for the case are all within 4% from each other[4]. Therefore, it must be understood that the RELOAD-Ⅱ-predicted fuel loading pattern is not the optimum one in the strictest sense of the word, but the near-optimum one.

3.4. Depletion Analysis for Fuel Cycles 2-5.

The depletion computation for full power and reactivity-limited burnup is performed for the second cycle of the Gori reactor with the fuel loading pattern as determined in the above. The same computation is also carried out for the fuel cycles up to the 5th, using the TDCORE code. The EOC burnup distribution of each fuel cycle is used as the input for determining the optimum fuel loading pattern of the succeeding cycle by the RELOAD-Ⅱ code.

Shown in Figs. 12-15 are the results of the power and burnup computations for the cycles 2 through 5. The BOC fuel loading

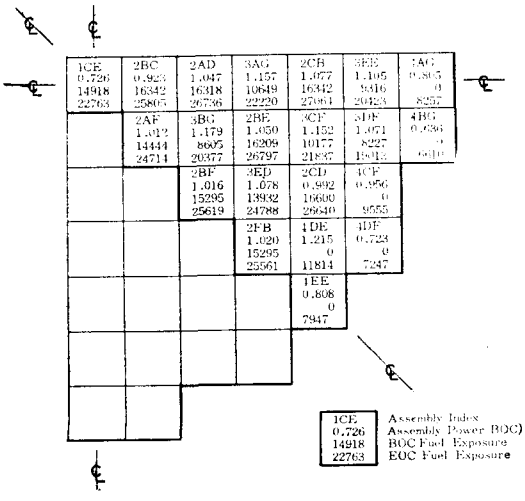

Fig. 12. Burnup Performance of Fuel Assemblies in the Second-cycle Gori Core

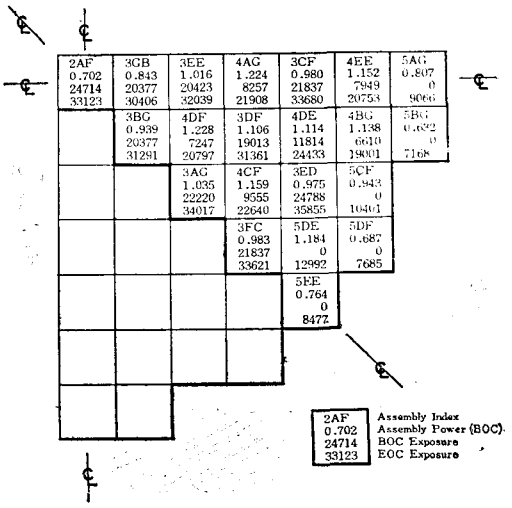

Fig. 13. Burnup Performance of Fuel Assemblies in the Third-cycle Gori Core

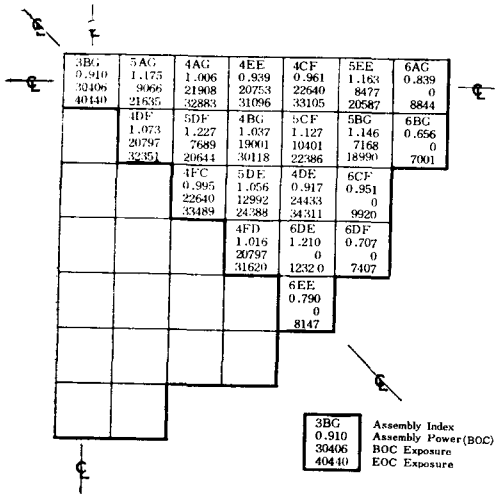

Fig. 14. Burnup Performance of Fuel Assemblies in the Fourth-cycle Gori Core

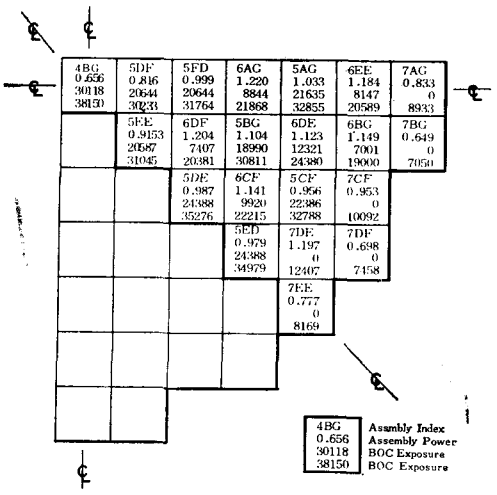

Fig. 15. Burnup Performance of Fuel Assemblies the Fifth-cycle Gori Core

Table 4. Cycle-by-Cycle Critical Boron Concentration with Fuel Exposure
(C_B: Critical Boron Concentration in ppm)

Cycles \ Burnup (MWD/MTU) / Item		0	150	1000	3000	6000	9000	EOC
2	C_B	1525.4	1259.9	1144.6	906.9	588.2	233.3	51.30
	keff	.99992	.99992	.99990	1.0001	1.0000	.99993	.99998
3	C_B	1445.4	1184.6	1089.8	874.5	561.6	273.4	49.97
	keef	1.0001	1.0001	1.0000	1.0000	1.0001	1.0001	.99995
4	C_B	1390.6	1128.2	1016.9	797.3	489.2	198.8	49.11
	keff	1.0001	1.0001	1.0001	1.0000	1.0000	1.0000	1.0000
5	C_B	1416.5	1152.9	1039.5	817.6	507.6	214.9	49.52
	keff	1.0001	1.0000	1.0001	1.0000	1.0000	1.0001	1.0001

pattern, assemblywise BOC and EOC burnups, and BOC power peaking factors are included in these figures. In Table 4 is listed the variation of the critical boron concentration with the core burnup for the cycles 2 through 5. In Table 5 and 6 are summarized the burnup performance and mass data of the individual fuel batch by cycle. Like the second cycle, each succeeding fuel cycle is assumed to terminate at the core state with the critical boron concentration of roughly 50 ppm. In these tables are also listed the burnup data prepared by KECO for its long-term fuel procurement activity[12] given in the parentheses. Upon comparision of KECO data with the TDCORE predictions it is observed that the TDCORE code underestimates the batchwise fuel burnup and the average cycle burnups.

In Fig 16 is shown the movement of the individual fuel assembly from its initial loading to the final discharge from the core. The number in circle stands for the cycle number when the fuel assembly is initially charged into the core. The number attached to each arrow denotes the cycle number

Table 5. Cycle-by-Cycle Batchwise Fuel Burnup

Batch	Cycle						Discharge Burnup
	1	2	3	4	5	6	
1A	16310 (15800)						16310 (15800)
1B	14918 (15800)	7845 (9700)					22763 (25500)
2A	16004 (16750)	10272 (10250)					26276 (27000)
2B	14444 (16750)	10270 (10250)	8409 (9510)				33123 (36500)
3A	10225 (11450)	11270 (11100)	11519 (10150)				33014 (32650)
3B	8605 (11450)	11772 (11100)	10029 (10150)	10034 (9700)			33014 (32650)
4A		8719 (9400)	12989 (11450)	10689 (10600)			40440 (42350)
4B		6610 (9400)	12391 (11450)	11117 (10600)	8032 (9600)		32397 (31450)
5A			9448 (9550)	12078 (11800)	10863 (10400)		38150 (41050)
5B			2689 (9550)	12955 (11800)	9589 (10400)	8069 (9600)	32389 (31700)

Table 6. The Fuel Mass Data of the Gori Fuel Cycles

Batch No.	No. of Fuel Ass.	Average Burnup (MWD/MTU)	Fuel Loaded		Fuel Discharged			
			Uranium (MTU)	Enrichment (w/o)	Uranium (MTU)	Enrichment (w/o)	Fissile Pu (kg Pu)	Total Pu (kg Pu)
1A	40	16310 (15800)	16.040	2.122	15.674 (15.670)	0.9058 (0.93)	82.5 (81)	105.9 (105)
1B	1	22763 (25500)	0.401	2.122	0.387 (0.387)	0.6595 (0.55)	2.3 (2)	3.1 (3)
2A	39	26226 (27000)	15.639	2.835	15.069 (15.062)	0.9644 (0.91)	100.7 (100)	133.6 (136)
2B	1	33123 (36500)	0.401	2.835	0.382 (0.382)	0.6752 (0.59)	2.7 (3)	3.6 (4)
3A	39	33014 (32650)	15.639	3.199	14.958 (14.957)	0.9781 (0.91)	108.0 (108)	148.3 (149)
3B	1	40440 (42350)	0.401	3.199	0.380 (0.379)	0.6290 (0.59)	2.6 (3)	3.8 (4)
4A	39	32397 (31450)	15.639	3.2	14.959 (14.979)	0.9272 (0.96)	102.2 (107)	139.4 (164)
4B	1	38150 (41050)	0.401	3.2	0.381 (0.380)	0.7454 (0.62)	2.6 (3)	3.7 (4)
5A	39	32389 (31700)	15.639	3.2	14.959 (14.974)	0.9340 (0.95)	100.9 (107)	138.1 (147)
5B	1	38302 (41350)	0.401	3.2	0.381 (0.380)	0.7521 (0.61)	2.5 (3)	3.6 (4)

when the fuel assembly is finally discharged. The overall trend of the assembly movement with the fuel cycle is observed to show the out-in reloading.

4. Conclusion

We have adopted the TDCORE code and

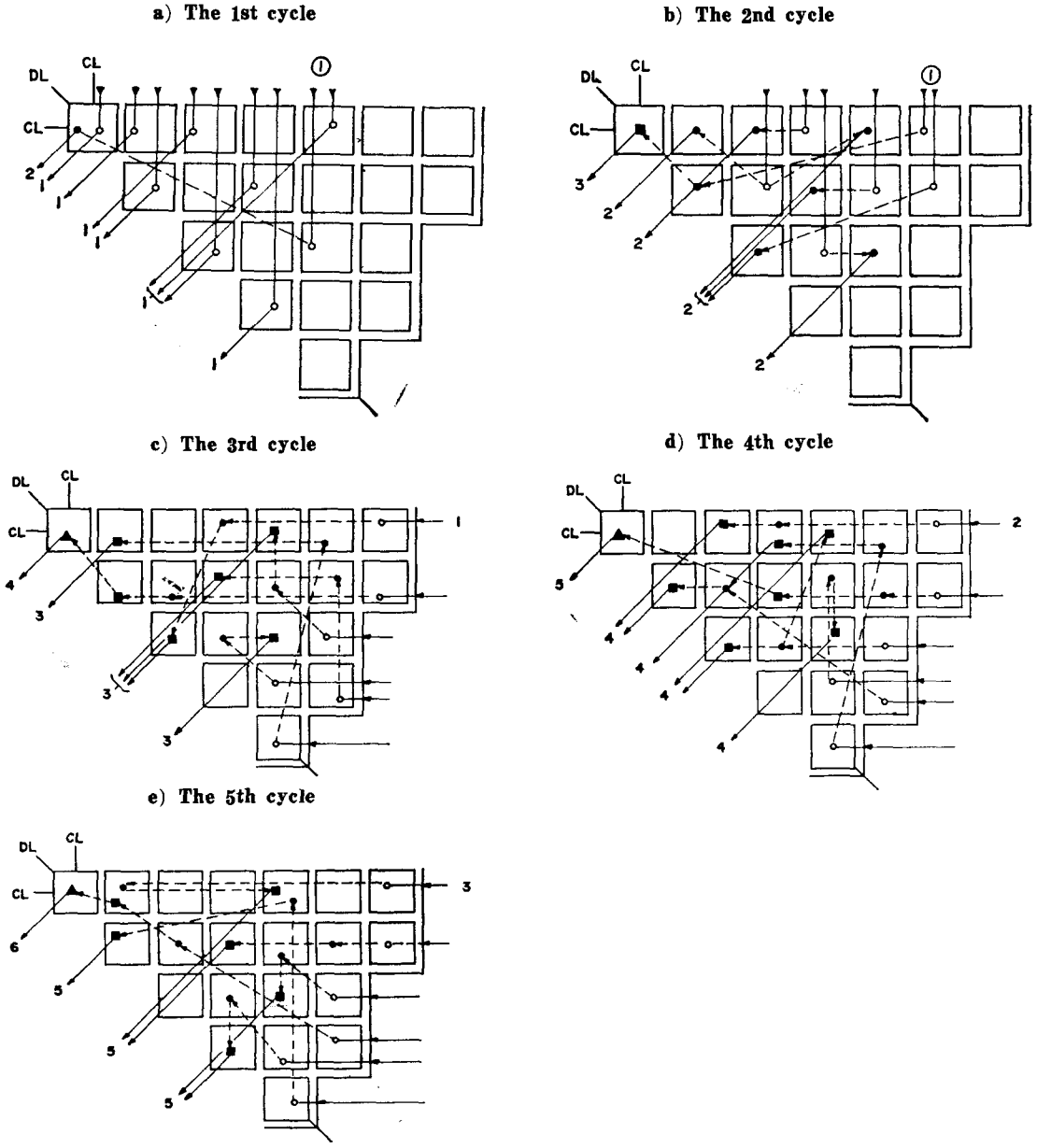

Fig. 16. Cycle-by-Cycle Assembly Movement from its Initial Load to the Final Discharge

the RELOAD-Ⅱ code for the simplified fuel management computations of the Gori unit 1 PWR. It is demonstrated that the TDCORE code can predict the cycle-by-cycle assemblywise power and burnup distributions and the critical boron concentration within an acceptable error bounds. The RELOAD-Ⅱ code is found useful for determining the optimal fuel loading pattern with respect to the minimum radial power peak. The optimality of the loading pattern determined by the RELOAD-Ⅱ code is not proven, yet the loading pattern obtained from it is considered an acceptable near-optimum one.

TDCORE and RELOAD-Ⅱ are very fast-

running computer codes. The computer running time of the TDCORE code is typically less than 30 seconds on the CDC CYBER-73 condition for completing the cycle depletion computations conducted at five or six burnup steps. The computer running time of the RELOAD-Ⅱ code is less than 100 seconds on the same computer for determining the optimum fuel loading pattern. Therefore. two codes can be applicable to a wide scope of fuel management computations in a reasonable computer time.

References

1) K. Chitkara and J. Weisman, *Nucl.Tech.*, **24**, 33 (1974)
2) T. Kubokawa and R. Kiyose, Proc. of Conf. on Computational Methods in Nuclear Engineering, CONF-750413 (1975)
3) T.O. Sauer, *Nucl. Sci. Eng.*, **46**, 274 (1971)
4) 김창효외 수인, "가압경수형 원자력발전소의 핵연료관리에 관한 연구" 문교부(1978)
5) S. Bøerrensen, *Nucl. Sci. Eng.*, **44**, 37 (1971); *Trans. Am. Nucl. Soc.*, **15**, 956 (1972)
6) R.B. Stout and A.H. Robinson, *Nucl. Tech*, **20**, 86 (1973)
7) "Final Safety Analysis Report for Kori Nuclear Power Plant Unit No. 1", Korea Electric Company (1976)
8) P.C. Kalambokas and A.F. Henry, *Nucl. Sci. Eng.*, **61**, 181 (1976)
9) T.B. Fowler et. al., Nuclear Reactor Core Analysis Code; CITATION, ORNL-TM-2496, Rev. 2 (1969)
10) 이창건외 수인, "핵설계변경에 따른 원자력발전소의 경제성 및 안전성분석", 한국원자력기술주식회사(1978)
11) Private Communication with the Korea Electric Company (KECO) (1978)
12) Private Communication with the Fuel Division of KECO.